

IM-LUT: Interpolation Mixing Look-Up Tables for Image Super-Resolution

Supplementary Material

Sampling	Size	PSNR
2^0 (Full LUT)	73.13GB	36.48
2^1	4.64GB	36.46
2^2	306.67MB	36.43
2^3	20.59MB	36.41
2^4	1.67MB	36.34
2^5	360.02KB	36.20
2^6	255.67KB	35.58

Table S1. Effect of lut sampling interval on storage size and PSNR for $\times 2$ SR on the Set5 dataset.

A. Additional Experiments

A.1. Effect of Sampling Intervals

To investigate the impact of LUT sampling intervals on the weight predictor f_w , we conduct experiments NLC combination by fixing the refiner f_r and varying the quantization levels of f_w . Table S1 summarizes the results for $\times 2$ super-resolution (SR) with LUT fine-tuning [3], highlighting the relationship between LUT size and PSNR.

As shown in Table S1, larger LUT sizes generally yield higher PSNR values, indicating that finer quantization enhances interpolation mixing precision and improves reconstruction quality. However, this comes at the cost of increased storage requirements, which can be impractical for memory-constrained scenarios.

To balance efficiency and quality, we adopt a sampling interval of 2^5 (Ours NLC), which offers a favorable trade-off. While lower intervals (e.g., 2^0 , 2^2) yield marginal PSNR improvements, they require significantly larger storage. Conversely, higher intervals (e.g., 2^6) reduce storage demands but degrade image quality. Our setting minimizes storage overhead while maintaining PSNR close to that of the full LUT, demonstrating that moderate LUT quantization effectively preserves SR performance without excessive memory consumption.

A.2. Various Combinations of IM-LUT

To further analyze IM-LUT, Fig. S1 illustrates the trade-off between performance and efficiency for different interpolation combinations on $\times 2$ SR using Set5. More complex combinations, such as NLCZ, achieve higher PSNR at the expense of increased computational cost. In contrast, NLC and NLZ provide a more balanced trade-off between quality and efficiency. These results highlight IM-LUT’s capability to enhance SR performance while maintaining computational feasibility for resource-constrained applications.

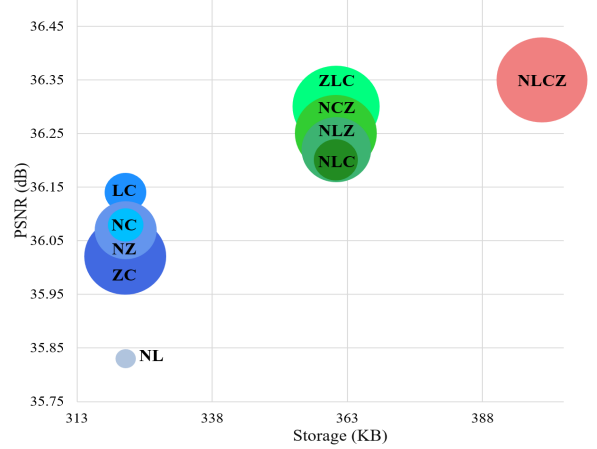


Figure S1. Performance-efficiency trade-off of different interpolation combinations with IM-LUT on $\times 2$ SR of Set5. The diameter of each circle is proportional to the MACs for producing a 1280×720 image.

A.3. Visualization Results

We further validate the effectiveness of IM-LUT through qualitative comparisons with interpolation-based methods and LeRF [2]. As shown in Fig. S4, our approach achieves superior texture reconstruction and edge sharpness for $\times 2$ SR on benchmark datasets compared to conventional interpolation and LUT-based SR models.

Additionally, we extend our analysis to ASISR methods, as shown in Fig. S2 and Fig. S3. IM-LUT consistently preserves text clarity and structural details at $\times 3$ and $\times 4$ magnifications, effectively mitigating blurring and artifacts observed in LeRF-G [2]. This highlights the strength of our adaptive interpolation mixing strategy, ensuring stable and visually coherent results even beyond the training distribution.

A.4. Explanation for Experiment Results

The results confirm that IM-LUT achieves strong performance across arbitrary scales with a single LUT set. Compared to fixed-scale methods like MuLUT and SPF-LUT, which require separate models for each scale, IM-LUT generalizes to both seen and unseen (including non-integer) scaling factors without retraining. Even when evaluated at the fixed scales those baselines are optimized for, IM-LUT shows comparable accuracy while being significantly more storage-efficient. This supports the effectiveness of our interpolation-based design and its favorable cost-accuracy trade-off compared to existing LUT-based approaches.

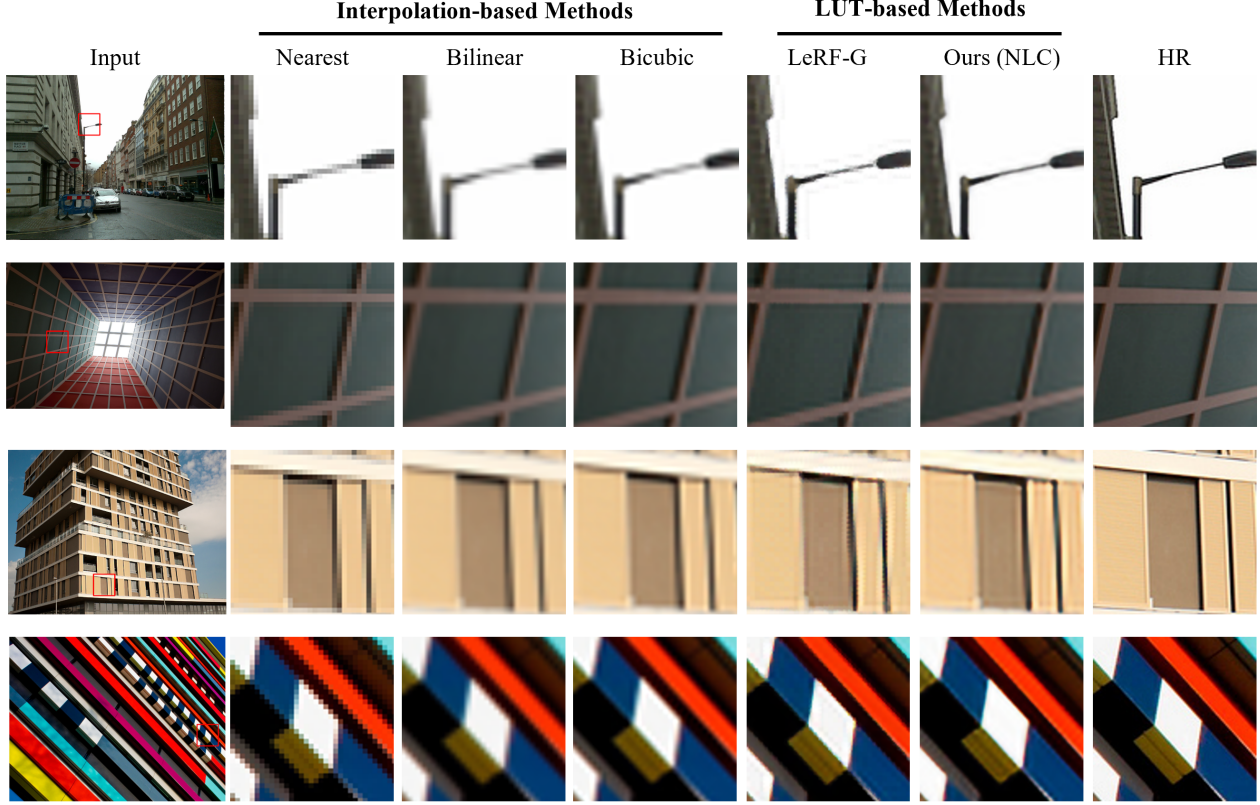


Figure S2. Comparison of $\times 3$ SR results of interpolation-based methods and LUT-based methods.

B. Details of IM-LUT

B.1. Rotation Ensemble

In practice, to expand the receptive field, we apply a rotation ensemble strategy [1] to both the weight predictor $f_w(\cdot)$ and the refiner $f_r(\cdot)$. The input patches are rotated by angles selected from the predefined set:

$$j \in \{0^\circ, 90^\circ, 180^\circ, 270^\circ\}. \quad (1)$$

For each rotated input, $f_w(\cdot)$ and $f_r(\cdot)$ generate corresponding outputs, which are aggregated to obtain the final predictions:

$$\mathcal{W} = \frac{1}{J} \sum_j f_w(R_j(\mathcal{I}_{LR})), \quad \mathcal{I}_{SR} = \frac{1}{J} \sum_j f_r(R_j(\mathcal{I}'_{SR})), \quad (2)$$

where J denotes the number of selected rotations.

By leveraging multiple rotated versions of the input, this strategy effectively expands the receptive field without increasing storage requirements.

Moreover, we employ a mixed-scale dataset for training, utilizing a total of seven scaling settings ranging from $\times 1.5$ to $\times 4.5$ in increments of 0.5. This diverse scale range not

only ensures that our model learns to handle arbitrary-scale super-resolution effectively but also enhances its ability to perform interpolation mixing by adapting to a wide variety of magnification factors. As a result, our method achieves improved flexibility and robustness in scale-adaptive SR.

B.2. Refiner Architecture

To enhance final output quality without increasing spatial resolution, we introduce a lightweight refiner designed with a directional ensemble structure. Unlike cascaded LUT architectures, our refiner operates in parallel, improving detail restoration while maintaining efficiency.

As the upscaling factor increases (e.g., $\times 2 \rightarrow \times 3 \rightarrow \times 4$), the Refiner accounts for only a modest portion of the total computational cost (17% to 20% MACs), demonstrating its practical overhead. This design choice allows IM-LUT to remain competitive in both accuracy and efficiency, as further evidenced in our main results and ablation studies.

References

- [1] Younghyun Jo and Seon Joo Kim. Practical single-image super-resolution using look-up table. In *Proceedings of*

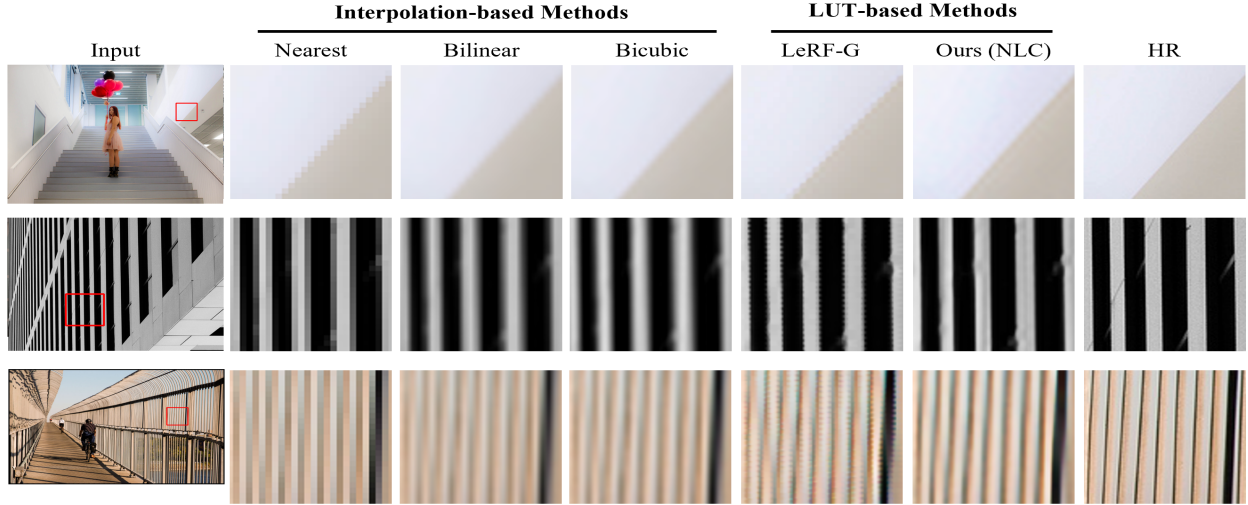


Figure S3. Comparison of $\times 4$ SR results of interpolation-based methods and LUT-based methods.

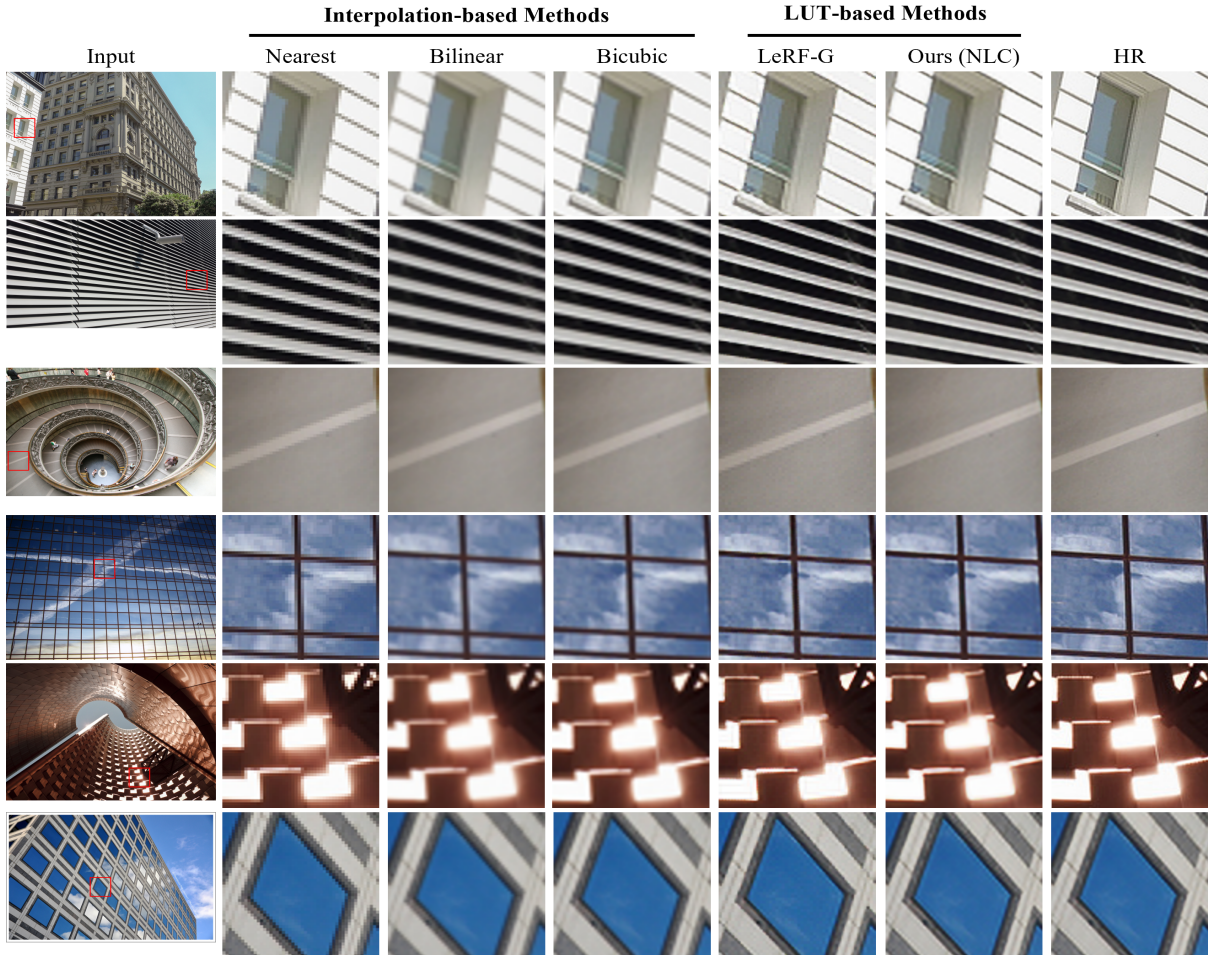


Figure S4. Comparison of $\times 2$ SR results of interpolation-based methods and LUT-based methods.

the IEEE/CVF Conference on Computer Vision and Pattern Recognition, pages 691–700, 2021. [2](#)

- [2] Jiacheng Li, Chang Chen, Wei Huang, Zhiqiang Lang, Fenglong Song, Youliang Yan, and Zhiwei Xiong. Learning steerable function for efficient image resampling. In *Proceedings of the IEEE/CVF Conference on Computer Vision and Pattern Recognition*, pages 5866–5875, 2023. [1](#)
- [3] Jiacheng Li, Chang Chen, Zhen Cheng, and Zhiwei Xiong. Toward DNN of LUTs: Learning efficient image restoration with multiple look-up tables. *IEEE Transactions on Pattern Analysis and Machine Intelligence*, 2024. [1](#)